Received: 14 October 2022 | Revised: 24 November 2022 | Accepted: 05 December 2022
DOI: 10.37917/ijeee.19.1.14 Vol. 19| Issue 1| June 2023

Open Access

Iraqi Journal for Electrical and Electronic Engineering
Original Article

New Design of a Compact 1×2 Super UWB-MIMO Antenna for Polarization Diversity

Watheq A. Neamah *[1,2], Haider M. Al Sabbagh[1], Hussain Al-Rizzo[3]
[1] Department of Electrical Engineering, College of Engineering, University of Basrah, Basrah, Iraq
[2] Biomedical Engineering Department, College of Engineering, University of Thi-Qar
[3] Department of Systems Engineering, University of Arkansas University Little Rock, Little Rock, USA

Correspondence
*Watheq Abdulkareem Neamah
Department of Electrical Engineering,
University of Basrah, Basrah, Iraq
Email: watheq.neamah@utq.edu.iq

Abstract
This paper proposes a new design of compact coplanar waveguide (CPW) fed -super ultra-wideband (S-UWB) MIMO antenna with a bandwidth of 3.6 to 40 GHz. The proposed antenna is composed of two orthogonal sector-shape monopoles (SSM) antenna elements to perform polarization diversity. In addition, a matched L-shaped common ground element is attached for more efficient coupling. The FR-4 substrate of the structure with a size of 23 × 45 × 1.6 mm^3 and a dielectric constant of 4.3 is considered. The proposed design is simulated by using CST Microwave Studio commercial software. The simulation shows that the antenna has low mutual coupling (|S21| < -20 dB) with |S11|<−10 dB, ranging from 3.6 to 40 GHz. Envelope correlation coefficient (ECC) is less than 0.008, diversity gain (DG) is more than 9.99, mean effective gain (MEG) is below - 3 dB and total active reflection coefficient (TARC) is less than -6 dB over the whole response band is reported. The proposed MIMO antenna is expected efficiently cover the broadest range of frequencies for contemporary communications applications.

KEYWORDS: Two Ports, MIMO, Super UWB, High Isolation, ECC, TARC.

I. INTRODUCTION

In recent years, antenna designs for not only ultra-wideband (UWB) applications (3.10 GHz-10.6 GHz), but also Super UWB (S-UWB) antennas with bandwidth ratios more than 10 to 1 have emerged as solutions for multiple applications, resulting in a new approach in wireless technologies such as microwave imaging, cognitive radio, sensing networks, higher data rate wireless communications, X-band Radar, and K-band Satellite [1], [2]. The demand for high data rates and good channel capacity has always been the top consideration in modern wireless communication systems. Wireless communication systems depend on ultra-wideband UWB and multi-input-multi-output (MIMO) technologies for high-speed data streaming [3]. Multipath fading is one of the main problems that degrade the performance of UWB systems, and it can be overcome using MIMO technology [4]. MIMO systems can use diversity to improve communication device reliability without requiring additional transmitted power or bandwidth by mitigating the vulnerable multipath fading issue [5]. MIMO antennas have received much attention recently as critical devices in UWB MIMO systems. Those UWB antennas are also successfully used in the Internet of Things (IoT) [6], the radar sector, the microwave and other applications, not restricted to new mobile technologies [7].

Practical UWB antenna design challenges include broad impedance matching, radiation stability, a low profile, and a cheap cost [8]. There are two major challenges in designing MIMO antennas for UWB systems. One major challenge for MIMO systems is to reduce antenna elements' size. The other is to make the antenna elements more isolated from each other [9]. It is important to note that UWB wideband impedance matching should be unaffected by the methods employed to decrease mutual coupling.

Within the last several years, many proposals for S-UWB antennas have emerged [10]–[13]. In [10], a CPW-fed slotted circular monopole achieves a bandwidth of (11.66-56.1) GHz. To achieve a frequency range of 3.32 to 20 GHz, a monopole structure made of circular corrugations on a defective ground is reported [11]. A bow-tie-shaped vertical patch with two asymmetrical ground planes to get bandwidth (3.035–17.39) GHz is proposed [12] . The suggested structure in [13] is a triangular patch fed by a CPW to achieve a bandwidth of 4.9-25 GHz.

Because of their ubiquitous usage in modern applications, S-UWB MIMO antennas have garnered much attention in recent years. Many studies have been conducted

to improve the isolations between and decrease the mutual coupling among the components of UWB MIMO antennas. Suppressing mutual coupling and offering an alternative current path are broad categories into which all methods may be conducted. When antennas are placed in an orthogonal configuration, there is a lot of space between each antenna element, which prevents interference [14], [15]. If the size of the antenna is not a major consideration in the design, this method can be used successfully. Also, the mutual coupling can be minimize by ground plane modifications, such as engraving slits, slots, and adding stubs, which promote isolation between elements by altering the distribution of surface currents [16]–[18]. Slits, slots, and stubs are examples of parasitic decoupling components whose form is crucial because of the frequency dependence of the structures [19]–[22].

The aim of this paper is to design a 1×2 super UWB MIMO antenna based on orthogonal polarization diversity. The proposed structure consists of two rotated orthogonal single-shape monopole antenna for optimal performance within a bandwidth of 3.6 to 40 GHz. In addition, the antenna is equipped to L-shape common ground for efficient coupling. The designed antenna is simulated by using CST software. The antenna's performance is determined in terms of main quantities, such as loss and gain, also MIMO metrics, such as ECC, MEG, and TARC. This paper is organized as follows. Section 2 describes the design procedure of a single patch, whereas the configuration of MIMO components is discussed in its subsection. In Section 3, the MIMO antenna analysis is presented in detail, while in Section 4, the findings are compared to earlier work in the field. Section 5 concludes with a summary of the noteworthy results.

II. Antenna Configuration

A. Design Procedure

Figure 1 shows the geometry of the UWB sector like shape monopole antenna. The overall size of UWB antenna is 20×27 mm printed on a ε_r 4.4, 0.0025 lost tangent and a 1.6 mm thick FR4 low cost substrate. The element proposed antenna consists of sector shape feed by coplanar waveguide. The primary design is started by calculating a radius of a circular patch antenna, as described by Equations (1,2) [23].

$$R = \frac{A}{1+\frac{2H}{\pi A \varepsilon_r}\left[\ln\left(\frac{\pi A}{2H}\right)+1.7726\right]^{1/2}} \quad (1)$$

$$A = \frac{8.791*10^9}{f_r\sqrt{\varepsilon_r}} \quad (2)$$

where

ε_r : Dielectric constant of the substrate

f_r : Resonant frequency, GHz

H: Thickness of the substrate, cm

However, the idea of merge large and tiny sectors of circles is to stimulate all resonance modes for various frequencies by co-linear their centers. To obtain bandwidth enhancement for UWB applications, a SSM is rotated with angle (RO) as parametric study to get better impedance bandwidth. The CST program is used for computer simulation design. A 50 Ω subminiature version A (SMA) connection is added to the simulated model for coupling matching to improve simulation precision. Table 1 shows the antenna's final optimized dimensions.

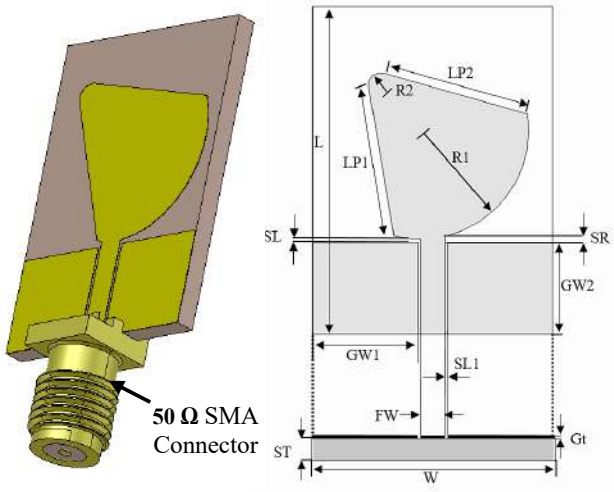

Fig.1: Schematic representation of proposed sector-shape monopole (SSM) UWB antenna element. The 50 Ω subminiature version A (SMA) connector is included for coupling matching. The values of dimensions can be found in Table I.

Figure 2 shows the rotating a sector-shaped patch across various degrees allowed us to examine its effect on impedance bandwidth. Figure 3 shows reflection coefficient across different angles of (RO). An optimal value is obtained at (RO) of 46 degrees to achieve a bandwidth of around 36.5 GHz (3.5- 40) GHz.

TABLE I
PROPOSED ANTENNA DIMENSIONS

Parameter	W	L	FW	R_2	GW1	Gt	GW2
Unit(mm)	18	23	2.5	7.5	50	0.035	7.5
Parameter	LP1	LP2	SR	SL_1	ST	SW	R_1
Unit(mm)	12.75	12.75	0.4	0.25	1.6	19	1

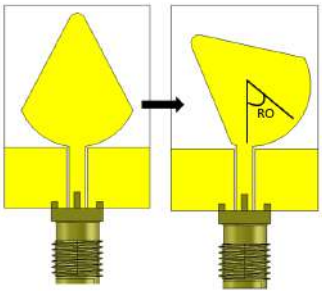

Fig. 2: UWB sector shape monopole (SSM) antenna (a) primary shape (b) final shape view.

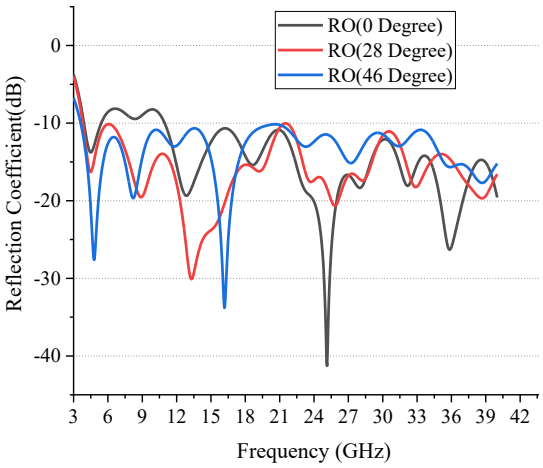

Fig. 3: Reflection coefficients versus frequency for different values of sector shape monopole (SSM) rotation angles (RO).

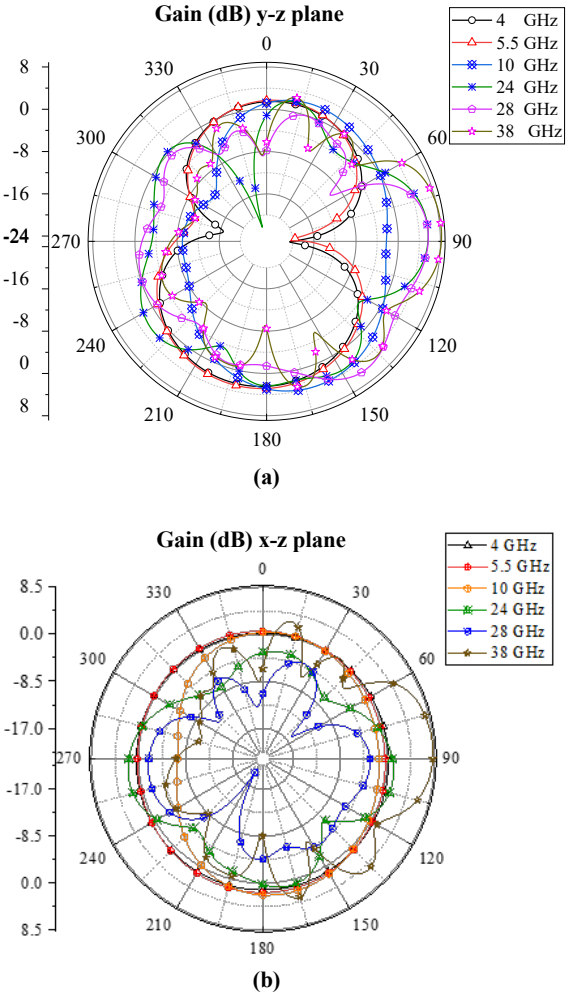

Fig. 4: Simulated gain of proposed super UWB single patch antenna at frequencies 4, 5.5, 10, 24, 28, and 38 GHz (a) y- z plane (b) x-z plane.

As shown in figure 4, we modelled the suggested design's 2-D radiation patterns at five of the most modern usable frequencies: 4, 5.5,10, 24, 28, and 38 GHz. In figure 4 (a), the suggested design shows an "8" pattern shape at low frequencies and a near-to-omnidirectional form at high frequencies on the y-z-plane, while in figure 4(b), the x-z-plane pattern resembles that of a near-to-omnidirectional form at low frequencies and near to "8" shape at high frequencies.

B. 1×2 MIMO Antenna Configuration Analysis

In this part, S-UWB-MIMO antennas are presented to achieve the polarization diversity principle by two identical sector-shape monopole patch antennas set orthogonally, as shown in figure 5. The MIMO antenna is a compact shape of 45×23×1.6 mm3, where the nearest separation between adjacent patches is $\lambda_0/11$, where λ_0 is calculated at 3.6 GHz at free space. The antenna is optimized by using the Computer Simulation Microwave Studio (CST MWS) software. First, it will refer to the sector patch state, either right or left side orientation depending on the arc position for its front view. The patches are enumerated as 1 and 2; as shown in figure 5, patch 1 is said to be the left layout, whereas patch 2 is the right layout. We investigated all cases of patch antenna layouts to get better isolation between antenna elements. Figure 6 depicts four scenarios of impedance bandwidth (S11&S22<-10) and isolation (S12 and S21) versus frequency, which depends on the cases of MIMO elements alignments. As shown in Figure 6 (a), for right-right configuration, the isolation reaches 15.6 dB and 17 dB of bands (9.3-13.5) GHz and (19.3-25.6) GHz, respectively, while the impedance bandwidth of S11&S22<-10 is between 3.6 to 40 GHz, again this isolation is not satisfied the MIMO optimal result. When the right-left configuration is considered, as shown in figure 6 (b), the isolation is confined between (9.3-13.5) GHz and (19.3-25.6) GHz, which have less than 20 dB. The impedance bandwidth of S11&S22<-10 is between 3.6 to 40 GHz, except S11 is notched at 7 GHz; again, this result does not satisfy good MIMO criteria. As shown in Figure 6 (c), for the left-left configuration, the frequency region 8.8 to 20.4 GHz has an isolation of less than 20 dB; once again, this isolation does not meet the criteria for MIMO. When the left-right configuration is considered, as shown in figure 6 (d), the isolation is more than 20 dB over the impedance bandwidth of (3.6-40) GHz.

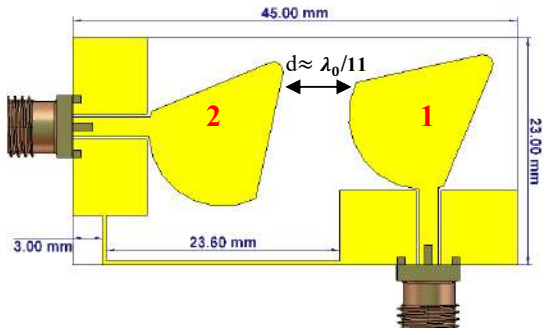

Fig. 5: Orthogonal two element MIMO antenna.

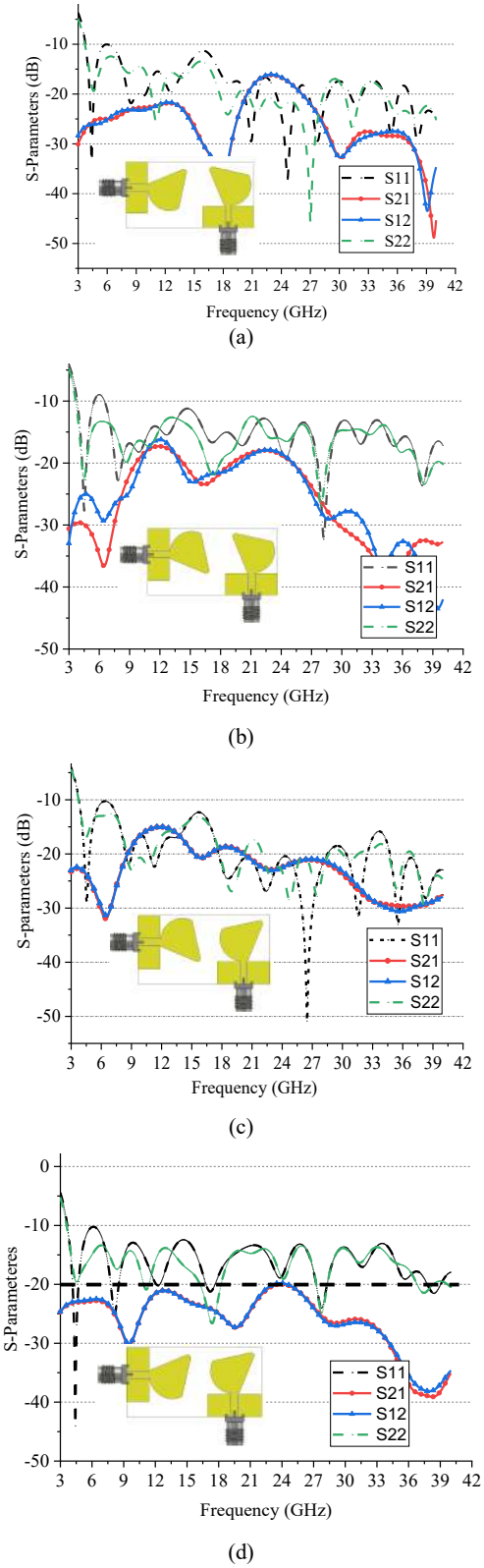

Fig. 6: Orthogonal two element MIMO antenna (a) (Right – Right) (b) (Right-left) (c) (Left –Left) (d) (Left –Right).

Antennas with a (left-right) layout can provide Super-UWB (3.6-40) GHz and achieve high isolation of more than 20 dB. To make the antenna applicable, we proposed an L-shaped common ground. However, in most cases, a common ground structure causes the resonance between this structure and the radiation elements, which causes rejects in its response. Figure 7 shows the S-parameters of the final shape of the 1×2 orthogonal MIMO antenna with L common ground by considering the left-right layout. Good results can be seen shown in figure 7, where the reflection coefficients of S11 and S22 are less than -10 dB for a frequency range of 3.6 to 40 GHz, with an isolation of less than 20 dB.

Figure 8 shows the simulated gain versus frequency. The minimum value recorded of the gain is about 1.6 dBi by CST software at 3.6 GHz, while the maximum value is obtained at 40 GHz, which equals 5.9 dBi. This gain is acceptable for most modern telecommunication applications.

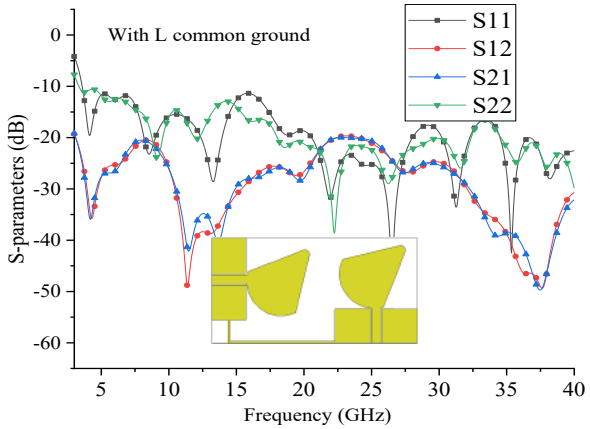

Fig. 7: S-parameters with L common ground of MIMO antenna versus frequency by using CST.

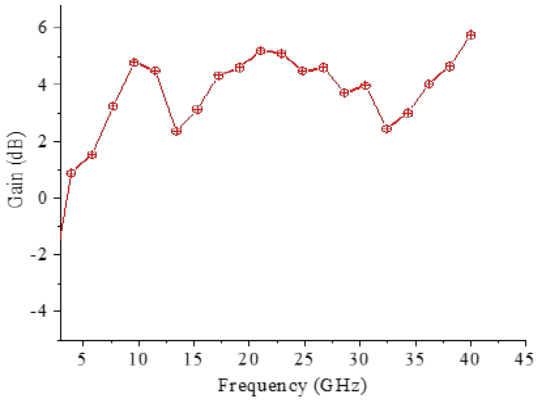

Fig. 8: Simulated gain of MIMO antenna versus frequency by using CST.

Figure 9 shows the simulated surface current versus different frequencies along the response band when port 1 is excited. As shown in figure 9, the current is concentrated around the patch's neck. Most of the current is along the arc and the angle side edge.

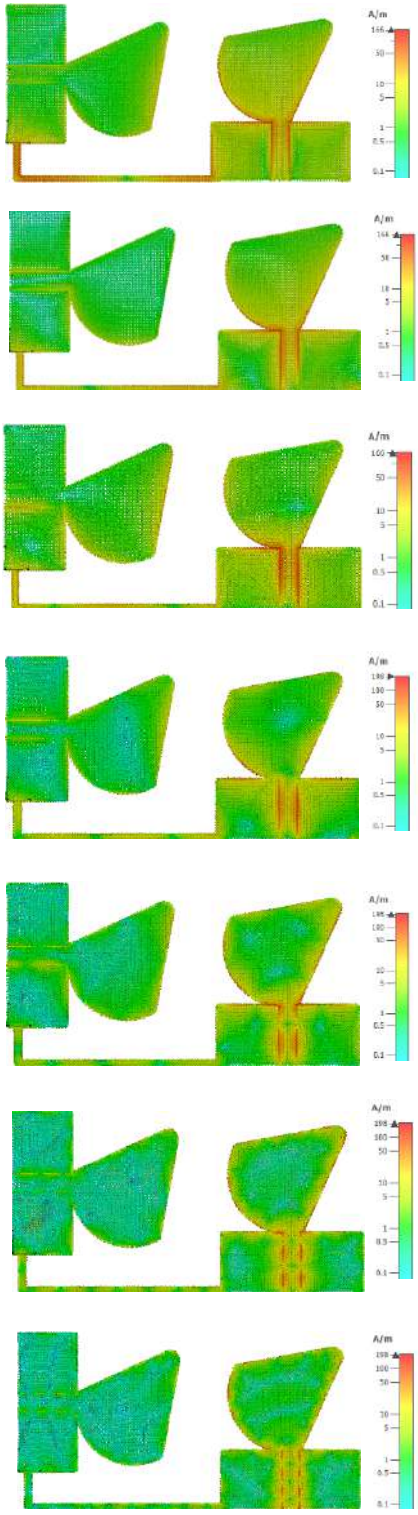

Fig. 9: The surface current distribution at different frequency when port 1 excited.

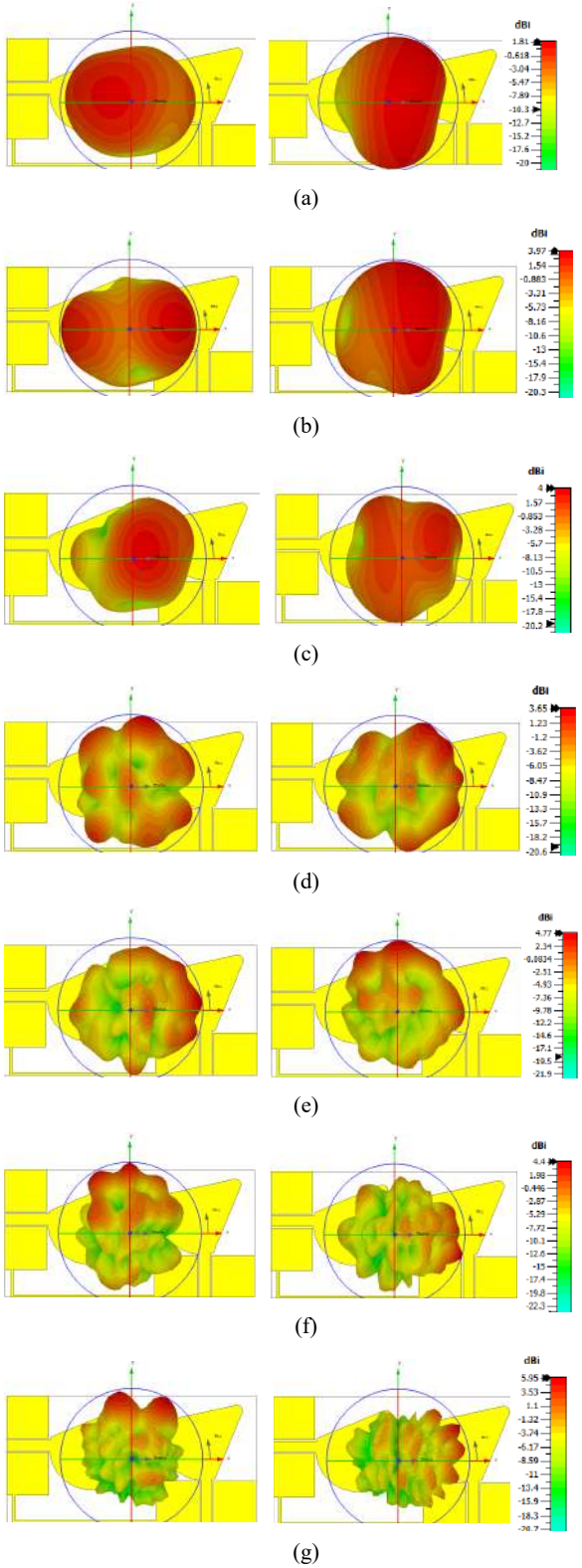

Fig. 10: The 3D radiation pattern at different frequencies (a) 4 GHz (b) 5.5 GHz (c) 8.5 GHz (d)18 GHz (e) 24 GHz (f)28 GHz (g) 38 GHz.

The isolation is enhanced when the second patch antenna is placed on the right instead of the first antenna, which is set on the left. The surface current flows in opposite directions in the orthogonal antenna because of the inconsistency of closed adjacent geometry antenna elements, especially for (left-right) layout; thus, this causes high isolation. This approach introduces self-decoupling by surface current and improves antenna isolation. Figure 10 shows the 3D radiation pattern over the response band at different frequencies. As shown in figure 10, the 3D radiation pattern MIMO antenna is simulated at frequencies 4, 5.5, 8.5,18,24,28 and 38 GHz. The complementary pattern of the two ports can be seen over the whole frequency response band.

III. Performance of Proposed MIMO Antenna

MIMO technology provides a new degree of freedom for wireless data communications and greatly enhances data transmission. The envelope correlation coefficient (ECC), diversity gain DG, mean effective gain MEG and total active reflection coefficient TARC are evaluated and presented to confirm the proposed MIMO antenna's diversity capability. The ECC is applied to determine the antenna element correlation. Law correlations between the antenna elements should be used to achieve greater diversity between the MIMO antenna elements. Acceptable ECC limits fall within a range of a maximum is 0.5 and may be calculated using Equation (3)[24] .

$$ECC = \rho_e = \frac{\left|S_{11}^{*}S_{12}^{\Diamond} + S_{21}^{*}S_{22}^{\Diamond}\right|^2}{\left(1-(|S_{11}|^2-|S_{21}|^2)\right)\left(1-(|S_{22}|^2-|S_{12}|^2)\right)} \quad (3)$$

where S_{11}^{*} and S_{21}^{*} represent the imaginary components of S_{11} and S_{21} parameters, respectively. $S_{12}^{\Diamond}$ and $S_{22}^{\Diamond}$ are real parts of the S_{11} and S_{21} parameters, respectively.
For a more precise calculation, we can calculate ECC by using the far field, which is given by Equation (4)[25]:

$$ECC(\rho_e) = \frac{\left|\iint 4\pi[R1(\theta,\Phi).R2(\theta,\Phi)d\Omega]\right|^2}{\iint 4\pi\,|R1(\theta,\Phi)|^2\,d\Omega \iint 4\pi\,|R2(\theta,\Phi)|^2\,d\Omega} \quad (4)$$

where $Ri\ (\theta, \emptyset)$ denotes the radiation pattern when port (i) is activated, and Ω denotes the solid angle.
The following approximate expression is used to calculate the diversity gain as given in Equation (5)[26].

$$DG = 10\sqrt{1-(\rho_e)^2} \quad (5)$$

Figure 11 depicts the ECC calculated with two methods; one is by using S-parameters, and the second is by using far-field versus frequency; also, DG is included in this figure. As shown in figure 11, the ECC<0.001 we get by S-parameters and ECC<0.007 by far-field shows outstanding system performance from 3.6 GHz to over 40 GHz. This result is quite less than the lime of MIMO condition. Furthermore, the antenna system has a high diversity gain (DG>9.99 dB) over the frequency range, producing a good performance.

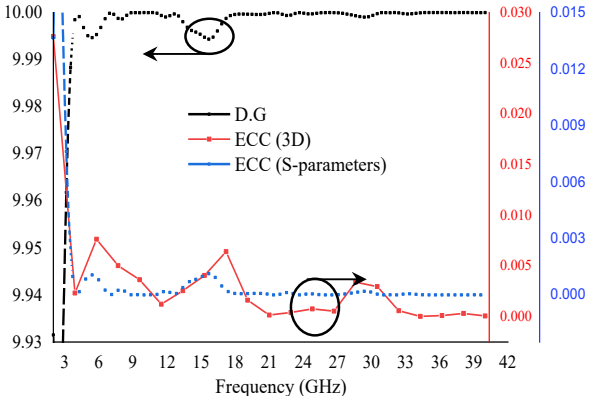

Fig.11: Envelope correlation coefficient (ECC) in both S-parameters and radiation pattern, including diversity gain (D.G) versus frequency.

The MEG is an important MIMO parameter investigated in this study. The MEG can define as the ratio of the average power received from the test antenna in the same environment to the average power obtained by a reference antenna. The ideal MEG value should fall between -3 and -12 dB for each. Equation (6) can be used to calculate MEG[27].

$$MEG_{(i)} = 0.5\left(1-\sum_{j=1}^{n}\left|S_{ij}\right|^2\right) \quad (6)$$

Where n is number of antennas, and for two ports MEG can be found by:

$$MEG_{(1)} = 0.5-|S11|^2-|S12|^2$$

$$MEG_{(2)} = 0.5-|S21|^2-|S22|^2$$

Furthermore, the ratio of MEG1/MEG2 is less than 3 dB for the optimal result to ensure good performance. Figure 12 shows the calculated MEG1, MEG2, and MEG1/MEG2. As shown in figure 12, EMG1 and EMG2 are close to the optimal value, which is -3dB, while their ratio is almost 0 dB, which implies conforming with optimal MIMO conditions.

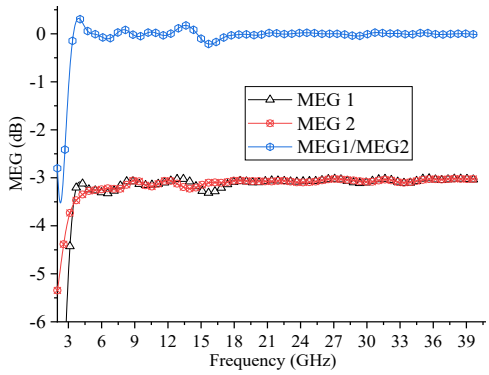

Fig. 12: Simulated mean effective gain MEG1, MEG2 and MEG1/ MEG2 versus frequency of the super-UWB-MIMO antenna.

The TARC is a crucial metric in calculating the interference or mutual coupling between MIMO antenna ports. It is possible to calculate the TARC for two-port MIMO antennas by considering the relationships between S11/S22 and S21/S12. A TARC value below 0 dB is desired with an uncorrelated MIMO antenna system. TARC can be calculated by Equation (7) [28].

$$TARC = \sqrt{\frac{(S_{11}+S_{12})^2+(S_{22}+S_{21})^2}{2}} \quad (7)$$

Figure 13 shows the calculated TARC. As shown in figure 13, the TARC is below -6 dB overall band response, which is consistent with the MIMO condition.

IV. Results Comparison

Table 2 compares two-port orthogonal 1×2 MIMO antennas already reported accordingly. One can see from the table that the overall results of our design are eminent either by bandwidth, gain, ECC, dimensions or isolation. However, the references are introduced in some with high isolation or low ECC, their limit either by dimensions or by design complexity. This comparison shows that our design besides having a simple design, the proposed MIMO antenna has high isolation, a good gain, and a low ECC.

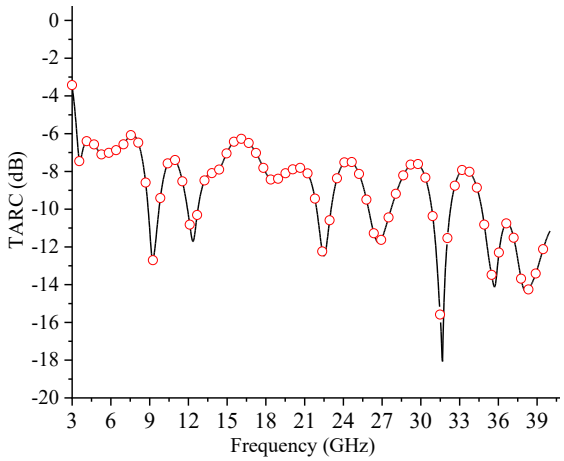

Fig.13: Total active reflection coefficient (TARC) of proposed antenna versus frequency of operation.

TABLE II
Previous Work Comparison

Ref No.	Dimensions MM^3	Isolation (dB)	B.W GHz	ECC	Peak Gain (dBi)
[29]	100×40×1.6	<30	5.5 –7.5	<0.001	-
[30]	45×45×1.59	<15	(3.28-3.72)(4.44-5.92)	<0.003	4.7/5.8
[31]	28×28×0.8	<20	(3.4-3.6) (4.8-5.0)	<0.003	2/2.46
[32]	29 × 29 × 0.8	<15	3.1–16.9	<0.017	4
This Work	45 × 23 × 1.6	<20	3.6-over 40	<0.008	5.9

V. Conclusion

Two ports S-UWB multiple-input multiple-output (MIMO) antennas based on polarization diversity have been proposed for modern communications. The antenna is designed to function at frequency bands ranging from 3.6 to 40 GHz, with isolation values more than 20 dB throughout the working frequency band. The single element is modified to resemble a sector-shaped monopole SSM patch antenna excited by the CPW feed technique and rotated with respect to its center. The MIMO array is aligned as orthogonal and investigated to perform self-decoupling with high isolation without using any structure. Common ground is proposed as an L-shape, which makes this MIMO antenna practical. The simulated design is achieved using CST software, modelled on an FR-4 substrate with a 4.3 dielectric constant. The overall array dimensions are 45×23×1.6 mm3. The MIMO metrics such as ECC, DG, TARC and MEG have been evaluated and give good MIMO performance. Simulation results within the intended operating ranges demonstrate that the recommended structure can be utilized for modern communications.

Conflict of Interest

The authors have no conflict of relevant interest to this article.

References

[1] T. Okan, "A compact octagonal-ring monopole antenna for super wideband applications," *Microw. Opt. Technol. Lett.*, vol. 62, no. 3, pp. 1237–1244, 2020, doi: 10.1002/mop.32117.

[2] S. Dey and N. C. Karmakar, "Design of novel super wide band antenna close to the fundamental dimension limit theory," *Sci. Rep.*, vol. 10, no. 1, pp. 1–15, 2020, doi: 10.1038/s41598-020-73478-2.

[3] W. Chien, C. Y. Yu, C. C. Chiu, and P. H. Huang, "Optimal location of the access points for MIMO-UWB systems," *Appl. Sci.*, vol. 8, no. 9, 2018, doi: 10.3390/app8091509.

[4] W. A. E. Ali and A. A. Ibrahim, "A compact double-sided MIMO antenna with an improved isolation for UWB applications," *AEU - Int. J. Electron. Commun.*, vol. 82, pp. 7–13, 2017, doi: 10.1016/j.aeue.2017.07.031.

[5] J. Ren, D. Mi, and Y. Yin, "Compact ultrawideband MIMO antenna with WLAN/UWB bands coverage," *Prog. Electromagn. Res. C*, vol. 50, no. April, pp. 121–129, 2014, doi: 10.2528/PIERC14041701.

[6] F. M. Alnahwi, K. M. Abdulhasan, and N. E. Islam, "An ultrawideband to dual-band switchable antenna design for wireless communication applications," *IEEE Antennas Wirel. Propag. Lett.*, vol. 14, no. c, pp. 1685–1688, 2015, doi: 10.1109/LAWP.2015.2418679.

[7] D. Minoli and B. Occhiogrosso, "Ultrawideband (UWB) Technology for Smart Cities IoT Applications," *2018 IEEE Int. Smart Cities Conf. ISC2 2018*, pp. 1–8, 2019, doi: 10.1109/ISC2.2018.8656958.

[8] P. Pannu and D. K. Sharma, "A low-profile quad-port UWB MIMO antenna using defected ground structure with

dual notch-band behavior," *Int. J. RF Microw. Comput. Eng.*, vol. 30, no. 9, pp. 1–13, 2020, doi: 10.1002/mmce.22288.
[9] S. P. Biswal and S. Das, "A compact dual port UWB-MIMO/diversity antenna for indoor application," *Int. J. Microw. Wirel. Technol.*, vol. 10, no. 3, pp. 360–367, 2018, doi: 10.1017/S1759078717001283.
[10] M. Rabiul Hasan, M. A. Riheen, P. Sekhar, and T. Karacolak, "Compact CPW-fed circular patch flexible antenna for super-wideband applications," *IET Microwaves, Antennas Propag.*, vol. 14, no. 10, pp. 1069–1073, 2020, doi: 10.1049/iet-map.2020.0155.
[11] D. Aissaoui, A. Chaabane, and A. Bouacha, "Compact Super UWB Elliptical Antenna with Corrugations for Wireless Communication Systems," *2020 1st Int. Conf. Innov. Res. Appl. Sci. Eng. Technol. IRASET 2020*, pp. 31–34, 2020, doi: 10.1109/IRASET48871.2020.9092221.
[12] R. Azim, M. T. Islam, H. Arshad, M. M. Alam, N. Sobahi, and A. I. Khan, "CPW-Fed Super-Wideband Antenna with Modified Vertical Bow-Tie-Shaped Patch for Wireless Sensor Networks," *IEEE Access*, vol. 9, pp. 5343–5353, 2021, doi: 10.1109/ACCESS.2020.3048052.
[13] M. Elhabchi, M. N. Srifi, and R. Touahni, "A Novel CPW-Fed Semi-Circular Triangular Antenna with Modified Ground Plane for Super Ultra Wide Band (UWB) Applications," *Int. Symp. Adv. Electr. Commun. Technol. ISAECT 2018 - Proc.*, pp. 1–5, 2019, doi: 10.1109/ISAECT.2018.8618857.
[14] D. K. Naji, "Design of a compact orthogonal broadband printed MIMO antennas for 5-GHZ ISM band operation," *Prog. Electromagn. Res. B*, vol. 64, no. 1, pp. 47–62, 2015, doi: 10.2528/PIERB15092104.
[15] V. S. D. Rekha, P. Pardhasaradhi, B. T. P. Madhav, and Y. U. Devi, "Dual Band Notched Orthogonal 4-Element MIMO Antenna with Isolation for UWB Applications," *IEEE Access*, vol. 8, pp. 145871–145880, 2020, doi: 10.1109/ACCESS.2020.3015020.
[16] A. McHbal, N. Amar Touhami, H. Elftouh, and A. Dkiouak, "Mutual Coupling Reduction Using a Protruded Ground Branch Structure in a Compact UWB Owl-Shaped MIMO Antenna," *Int. J. Antennas Propag.*, vol. 2018, 2018, doi: 10.1155/2018/4598527.
[17] L. Wang *et al.*, "Compact UWB MIMO Antenna with High Isolation Using Fence-Type Decoupling Structure," *IEEE Antennas Wirel. Propag. Lett.*, vol. 18, no. 8, pp. 1641–1645, 2019, doi: 10.1109/LAWP.2019.2925857.
[18] S. Kim and J. Choi, "Two-Port UWB MIMO Antenna with Modified Ground for Isolation Improvement," *ISAP 2018 - 2018 Int. Symp. Antennas Propag.*, no. Isap, pp. 914–915, 2019.
[19] A. Altaf *et al.*, "Isolation improvement in uwb-mimo antenna system using slotted stub," *Electron.*, vol. 9, no. 10, pp. 1–13, 2020, doi: 10.3390/electronics9101582.
[20] M. S. Khan, A. D. Capobianco, A. Iftikhar, R. M. Shubair, D. E. Anagnostou, and B. D. Braaten, "Ultra-compact dual-polarised UWB MIMO antenna with meandered feeding lines," *IET Microwaves, Antennas Propag.*, vol. 11, no. 7, pp. 997–1002, 2017, doi: 10.1049/iet-map.2016.1074.
[21] S. Chen, N. Lu, J. Sun, C. Zhou, C. Li, and D. Wu, "High-Isolation wideband MIMO antenna with offset T-Shaped slots for 5G/WLAN applications," *Front. Phys.*, vol. 10, no. August, pp. 1–10, 2022, doi: 10.3389/fphy.2022.986558.
[22] S. B. Paiva, A. G. D. Junior, V. P. S. Neto, and A. G. D'Assunção, "A New Compact Dual-Polarized MIMO Antenna Using Slot and Parasitic Element Decoupling for 5G and WLAN Applications," *Electronics*, vol. 11, no. 13, p. 1943, 2022, doi: 10.3390/electronics11131943.
[23] C. A. Balanis, *Constantine A. Balanis Antenna Theory Analysis*. 2005.
[24] C. Zhang *et al.*, "A Dual-Band Eight-Element MIMO Antenna Array for Future Ultrathin Mobile Terminals," *Micromachines*, vol. 13, no. 8, p. 1267, 2022, doi: 10.3390/mi13081267.
[25] X. L. Liu, Z. D. Wang, Y. Z. Yin, J. Ren, and J. J. Wu, "A compact ultrawideband MIMO antenna using QSCA for high isolation," *IEEE Antennas Wirel. Propag. Lett.*, vol. 13, pp. 1497–1500, 2014, doi: 10.1109/LAWP.2014.2340395.
[26] P. Palanisamy and M. Subramani, "Design of Metallic Via Based Octa-Port UWB MIMO Antenna for IoT Applications," *IETE J. Res.*, 2021, doi: 10.1080/03772063.2021.1892540.
[27] S. Tariq, S. I. Naqvi, N. Hussain, and Y. Amin, "A Metasurface-Based MIMO Antenna for 5G Millimeter-Wave Applications," *IEEE Access*, vol. 9, pp. 51805–51817, 2021, doi: 10.1109/ACCESS.2021.3069185.
[28] P. Prabhu and S. Malarvizhi, "Novel double-side EBG based mutual coupling reduction for compact quad port UWB MIMO antenna," *AEU - Int. J. Electron. Commun.*, vol. 109, pp. 146–156, 2019, doi: 10.1016/j.aeue.2019.06.010.
[29]R. G. Saadallah Alsultan and G. Ö. Yetkin, "Mutual coupling reduction of E-shaped MIMO antenna with matrix of C-shaped resonators," *Int. J. Antennas Propag.*, vol. 2018, 2018, doi: 10.1155/2018/4814176.
[30] J. Cai, J. Huang, B. Chen, L. Shen, T. H. Loh, and G. Liu, "A Defected Circular Ring Dual-Band MIMO Antenna with High Isolation for 5G and IEEE 802 . 11 a / ac / ax," vol. 113, no. October, pp. 237–247, 2022.
[31] G. Dong, J. Huang, S. Lin, Z. Chen, and G. Liu, "A Compact Dual-Band MIMO Antenna for Sub-6 GHz 5G Terminals," vol. 22, no. 5, pp. 599–607, 2022.
[32] H. Kaur, H. S. Singh, and R. Upadhyay, "A compact dual-polarized co-radiator MIMO antenna for UWB applications," *Int. J. Microw. Wirel. Technol.*, vol. 14, no. 2, pp. 225–238, 2022, doi: 10.1017/S1759078721000349.